Respuestas, 25 (3), September - December 2020, pp. ??-??, ISSN 0122-820X - E ISSN: 2422-5053

Respuestas
Journal of Engineering Sciences

Original Article https://doi.org/10.22463/0122820X.2936

A new methodology for detection of bearings faults in three-phase induction motor

Nueva metodología para la detección de fallas en rodamientos en motores de inducción trifásicos

Carlos Caceres-Amaya[1], Jorge Duarte-Forero[2*], Guillermo Valencia-Ochoa[3]

[1] Ingeniero de Sistemas, carloscaceres@gmail.com, ORCID: 0000-0001-7869-969X, Universidad Francisco de Paula Santander, Cúcuta, Colombia.
[2] Doctor en Ingeniería Mecánica, jorgeduarte@mail.uniatlantico.edu.co, ORCID: 0000-0001-7345-9590, Universidad del Atlántico, Barranquilla, Colombia.*
[3]Doctor en Ingeniería, guillermoevalencia@mail.uniatlantico.edu.co, ORCID: 0000-0001-5437-1964, Universidad del Atlántico, Barranquilla, Colombia.

Cómo citar: G. Caceres-Amaya, J. Duarte-Forero, G. Valencia-Ochoa, "A new methodology for detection of bearings faults in three-phase induction motor". *Respuestas*, vol. 25, no. 3, ??-??, 2020.

Received on June 22, 2020 - Approved on October 23, 2020.

ABSTRACT

This study shows a methodology for the detection, classification, and location of bearings that presented ball faults, cage faults, and outer race faults. For this study, a three-phase induction motor was used, in which the stator current and voltage signals were measured. By calculating the total harmonic distortion and using the Stockwell Transform, different characteristics were obtained in the electrical signals that allowed defining fault conditions in the bearing, classification of the type of fault, and the location of the defective bearing (fan side or load side). By calculating the difference between the total harmonic distortion of the current and voltage signal, it is possible to identify a threshold value of 0.004 that separates a healthy condition and a fault condition. The joint use of the Stockwell Transform and the Fisher Scoring Algorithm allows us to classify the fault conditions with an average precision of 92.5%. The location of a bearing with defects on the load side generates a greater amplitude in the signal compared to those located on the fan side. This behavior allows establishing a threshold value of 1.6 for ball faults and 0.001 for cage faults and outer race. Due to the results obtained, the algorithm proposed in the study is considered to be a tool with a high degree of reliability for the diagnosis of bearings in induction motors.

Keywords:
Bearing fault; Diagnosis; Induction motor; Stockwell transform; Three phases.

RESUMEN

Este estudio expone una metodología para la detección, clasificación y ubicación de fallas en rodamientos de bola, en la jaula y la pista exterior. Para este estudio se utilizó un motor de inducción trifásico, en el que se midieron las señales de tensión y corriente del estator. Calculando la distorsión armónica total y utilizando la Transformada de Stockwell, se obtuvieron diferentes características en las señales eléctricas que permitieron definir las condiciones de falla en el rodamiento, la clasificación del tipo de falla y la ubicación del rodamiento defectuoso (lado ventilador o lado carga). Calculando la diferencia entre la distorsión armónica total de la señal de corriente y voltaje, es posible identificar un valor de umbral de 0.004 que separa una condición de operación normal y una condición de falla. El uso de la Transformada de Stockwell y el algoritmo de puntuación de Fisher nos permite clasificar las condiciones de falla con una precisión promedio del 92.5%. La ubicación de un rodamiento con defectos en el lado de carga genera una mayor amplitud en la señal, en comparación con los ubicados en el lado del ventilador. Este comportamiento permite establecer un valor umbral de 1.6 para fallas de bola y 0.001 para fallas en la jaula y en la pista exterior. Por los resultados obtenidos, el algoritmo propuesto en el estudio se considera una herramienta con un alto grado de confiabilidad para el diagnóstico de rodamientos en motores de inducción.

Palabras clave:
Diagnóstico; Falla en rodamiento; Motor de inducción; Transformada de Stockwell; Trifásico.

Introduction

Electric induction motors are used repeatedly in industry, commerce, and the tertiary sector due to the advantages they possess, such as robustness, complete structure, easy control, and reliability [1] - [4]. In spite of having a relatively uncomplicated structure, induction motors are still exposed to different types of faults, including end ring faults, bearings, manufacturing defects, and broken rotor bars [5] - [9]. These faults can be associated with grounding problems, overloads, phase desynchronization, short circuits, and asymmetrical power supply [5], [10] - [14].

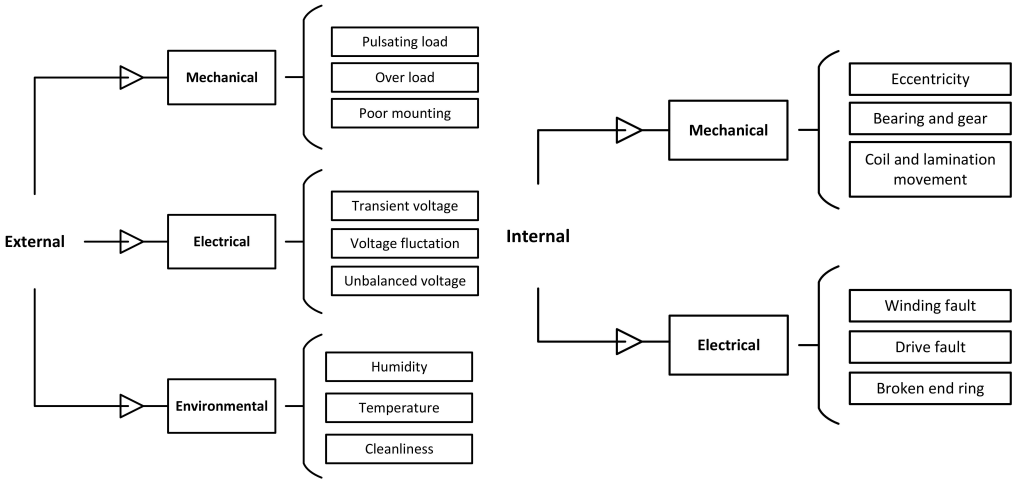

Figure 1. Faults (a) External and (b) Internal in induction motors.
Source: Authors, 2020.

The appearance of motor faults causes irregular operation, which leads to energy losses and increased maintenance work, which increases the economic costs of keeping the motor running. This shows the importance of early detection of faults in induction motors [1].

Among the most commonly used induction motors are squirrel cage motors. The types of faults that occur can be grouped into external and internal faults. Figure 1 shows a list of these two groups [15], [16].

In general, induction motors are exposed to high-temperature environments, corrosion, and mechanical stress. These conditions favor the development of incipient faults that are difficult to detect. This type of incipient fault does not cause a relevant problem to the engine. However, over time it can get worse and cause the engine to stop completely. Therefore, there is a need for methodologies that allow for monitoring conditions and early detection of faults.

In addition to energy losses, studies indicate that motor faults cause a greater tendency to experimental oscillations, voltage and current imbalances, power reduction, and overheating. Figure 2 shows the most common types of faults in induction motors [17].

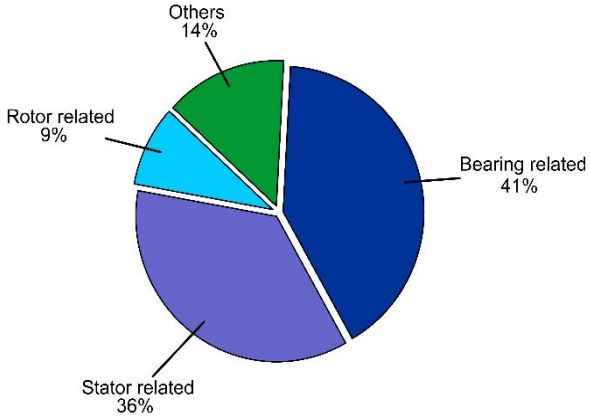

Figure 2. Typical faults in induction motors.
Source: Authors, 2020.

As shown in Figure 2, the bearings are the main fault in the motors. These faults are associated with broken cages, inner race, outer race, eroded balls, and among others. In general, vibration analysis is the technique used for bearing fault detection [18], [19]. This type of analysis requires the use of vibration transducers and modules, which makes it a costly analysis. An alternative is the motor current signature analysis (MCSA) since it only requires current measurements. In the case of the MCSA, the use of the Fourier Transform provides current signal spectrum information as a function of frequency for fault detection [20]. The spectral characteristic analysis is used for fault detection in multi-agent systems [21], [22]. Fast Fourier Transform (FFT) is the most frequently used tool for spectral analysis. However, it provides information without a time position, which can make the diagnosis of faults difficult.

More advanced signal processing techniques involving frequency and time domain can be used to overcome the shortcomings of FFT [23]. These techniques include the Short-Term Fourier Transform (STFT), the Hilbert-Huang Transform, the Wigner-Ville Distribution (WVD), and the Wavelet Transform (WT) [24], [25]. The techniques using STFT and WVD are limited by the presence of cross-terms and fixed window sizes. However, the WT technique overcomes these limitations. Therefore, the latter has been investigated to replace diagnostics based on current and vibration signals.

The Stockwell Transform (ST) is an enhancement of the Continuous Wavelet Transform (CWT), which allows for more information in the specific frequency bands. Several investigations have used ST in distribution systems using renewable energy sources and in transformer protection systems [26], [27]. Research by Singh and Shaik [28] shows that by analyzing the ST, it is possible to diagnose bearing faults. In this investigation, a methodology is proposed for the detection, classification, and location of bearings that presented ball faults, cage faults, and outer race faults. For this study, a three-phase induction motor was used, in which the stator current and voltage signals were measured, which were analyzed by calculating the total harmonic distortion and using the Stockwell Transform.

Materials and methods

Experimental bench description

For the experimental study, a 380V, 4-pole, 50Hz, three-phase induction motor was used. The motor shaft is supported by two types of bearings, 6205 and 6204, which are located on the load side and on the fan side. The motor characteristics are shown in Table I. A multimeter, a current module, and a voltage module were used to measure the electrical parameters of the motor. The measuring instruments are connected to a computer for the recording and subsequent analysis of the data. Figure 3 shows the connection diagram of the experimental bench of the motor.

Table I. Motor specifications

Parameter	Value
Model	ATO-Y2-90L-4
Insulation class	Class F
Nominal output	1.5 kW
Pole number	4-pole
Nominal speed	1400 rpm
Frequency	50 Hz
Nominal voltage	380 V
Nominal torque	10.2 Nm
Noise Level	61dB/(A)

Source: Authors, 2020.

Figure 3. Experimental test bench.
Motor controller, 2. Induction motor, 3. Multimeter, 4. Voltage module, 5. Current module, 6. Computer.
Source: Authors, 2020.

Three types of faults were selected for the study of bearing problems; cage fault, ball fault, and outer race fault. For each type of fault, 10 bearings were used to obtain the experimental samples. Additionally, experimental tests were carried out with 10 new bearings.

Experimental methodology

The measured stator currents for each test condition are analyzed in two ways. For the first analysis, the Fast Fourier Transform is used to identify the bearings that show some type of fault. Subsequently, the Stockwell Transformation is used to classify each type of bearing fault. Total Harmonic Distortion (THD) analysis was used to compare healthy and faulty bearings. With the use of the Stockwell Transformation, the characteristics of each type of fault are analyzed based on the statistical information of the magnitude and phase graphs.

The information about the characteristics of each test obtained with the analysis by FFT and ST are unified to build a matrix. The characteristics obtained are classified using the Fisher Score algorithm. The functions are then sent to a support vector machine (SVM) for function identification. The algorithm used in the present study consists mainly of three steps; fault detection, function selection for fault type identification, and fault bearing position location (fan side or load side).

Fault detection

To identify whether a bearing is in a healthy or fault condition, the total harmonic distortion is calculated using the FFT. The calculation obtained is compared with a reference value obtained from tests with healthy bearings. The calculation of this fault factor is shown in equation (1).

$$F_1 = THD_{current} - THD_{voltage} \qquad (1)$$

By means of the Stockwell transformation, a matrix was constructed consisting of rows representing changes in time and columns representing changes in frequency. Different statistical parameters are calculated from the data collected from the matrix.

Fisher's scoring criteria are used to classify the different characteristics. Because three types of bearing faults are studied, two SVM is used, identified as SVM-A and SVM-B. The fault identification scheme using the SVM is shown in Fig. 4.

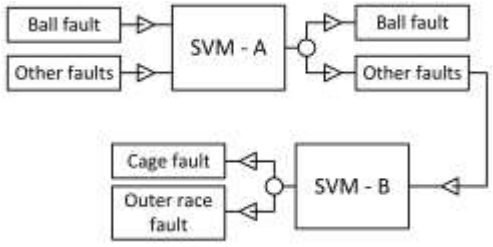

Figure 4. Fault classification using SVM.
Source: Authors, 2020.

Fault bearing position location

A bearing with a fault condition can be located on the fan side or on the load side of the motor. Two parameters are used to identify the location of the bearing, depending on the type of fault. In the case of ball faults, the maximum magnitude is calculated using equation (2).

$$F_2 = \max(max(|S(\tau, f)|)) \qquad (2)$$

Similarly, for the outer race fault and the cage fault, the maximum phase angle is calculated using equation (3).

$$F_3 = \max(max(|\phi(\tau, f)|)) \qquad (3)$$

The parameters calculated with equations (1) and (2) are compared with the respective threshold values. Figure 5 shows the scheme of the algorithm used in this study.

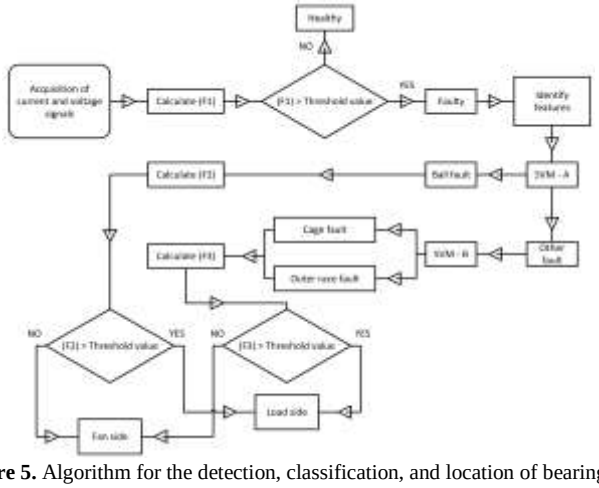

Figure 5. Algorithm for the detection, classification, and location of bearing faults.
Source: Authors, 2020.

Results and Discussion

Bearing fault detection

Figure 6 shows the Fast Fourier transform of the stator current signal for healthy bearings and those with cage defects.

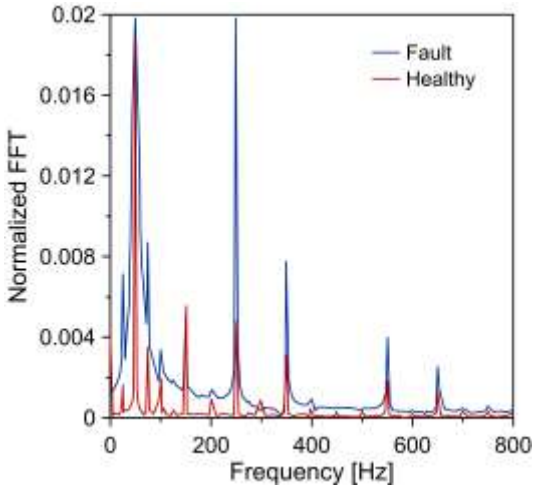

Figure 6. Fast Fourier Transform of the current signal.

Source: Authors, 2020.

It is observed that the presence of the bearing fault tends to produce signals with higher amplitudes along the frequency spectrum. However, the results obtained from the Fast Fourier Transform do not allow a clear determination of the healthy and fault condition. To solve this problem, the fault index (F1) is calculated, which was described in equation (1). With this fault index, the two bearing conditions are again compared. This comparison is shown in Fig.7

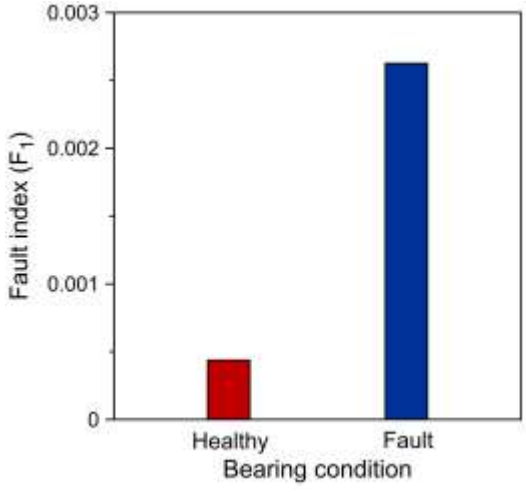

Figure 7. Fault index (F1) for each bearing condition.
Source: Authors, 2020.

By calculating the fault index (F1), an undeniable difference was observed between a bearing with a defect and a healthy one. The results show that the amplitude of the signal in the fault condition is six times greater than the healthy state. Due to these results, the fault index (F1) is recognized as a key tool to detect the presence of faults. In order to assess the capacity of the fault index (F1), the three bearing defects are individually compared to healthy conditions. The results obtained are shown in Fig. 8.

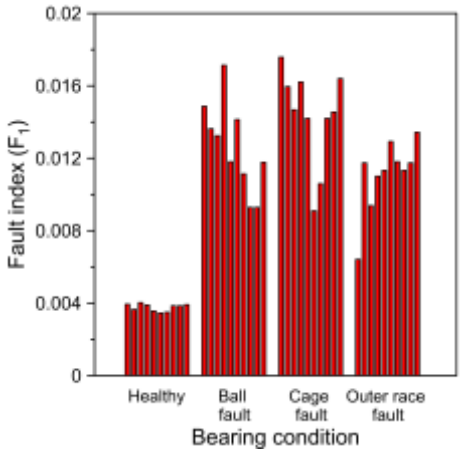

Figure 8. Fault index (F1) comparison for the three bearing fault conditions.
Source: Authors, 2020.

Figure 8 shows the fault index (F1) of the 10 bearings in each category (healthy, ball fault, cage fault, and outer race fault). Each of these defects produces a different range in signal amplitude. For the ball, cage, and outer race faults, mean amplitudes of 0.012, 0.014, and 0.011 were observed. However, for the healthy condition, the variability of the signal amplitude was less compared to the fault conditions. In all health conditions, the amplitude remained close to 0.004. Furthermore, in no-fault condition was the signal amplitude less than or equal to 0.004. Due to these two characteristics, it is possible to consider this value as a threshold for the detection of bearings with defects.

Selection of the main features of the signal

The collected characteristics of the 40 bearings are grouped into two databases. The first base is used to feed the SVM-A, and the second is used in the SVM-B. For testing, a linear SVM is chosen since it allows a higher speed of convergence and requires a lower computational cost.

By using the five characteristics shown in Table II, it was possible to achieve 95% accuracy in identifying ball fault or other types of fault. Fig.9 shows the accuracy of the SVM-A for different combinations of the five characteristics. In this case, 95% accuracy is achieved with a combined level of 335.

Table II. Diagnostic features used in the SVM-A

Feature	Equation
Kurtosis of Magnitude matrix	$Kurtosis\ (S(\tau,f))$
Standard deviation of magnitude matrix	$Std\ (S(\tau,f))$
Mean of Phase Angle matrix	$Mean\ (\angle S(\tau,f))$
Maximum of Magnitude matrix	$max\ (\lvert S(\tau,f)\rvert)$
Kurtosis of Phase matrix	$Kurtosis\ (\angle S(\tau,f))$

Source: Authors, 2020.

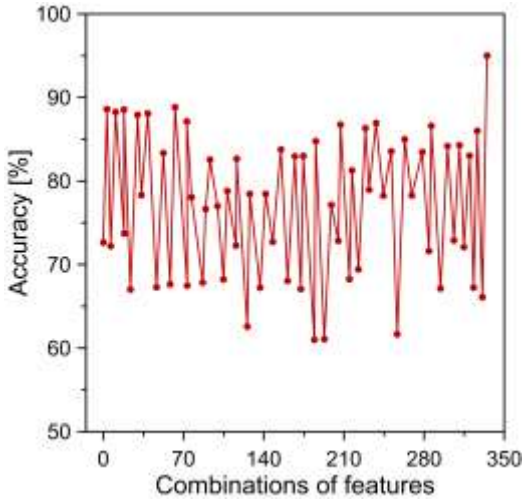

Figure 9. Accuracy for combinations of five characteristics used in SVM-A.
Source: Authors, 2020.

Similarly, in the case of the SVM-B, a maximum precision of 90% was obtained with the use of the three characteristics shown in Table III. This precision allows the identification of cage fault or outer race fault. Fig.10 shows that 90% accuracy is achieved with a combined level of 60.

Table III. Diagnostic features used in the SVM-B

Feature	**Equation**
Maximum of Phase matrix	$max\left(\angle S(\tau,f)\right)$
Kurtosis of Magnitude matrix	$Kurtosis\left(S(\tau,f)\right)$
Standard deviation of Phase matrix	$Std\left(\angle S(\tau,f)\right)$

Source: Authors, 2020.

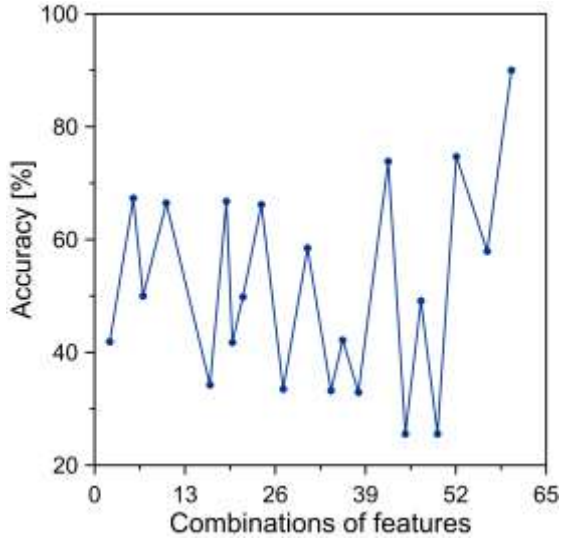

Figure 10. Accuracy for combinations of three characteristics used in SVM-B.
Source: Authors, 2020.

Faulty bearing location

The last step of the algorithm proposed in this study is to determine the location of the bearing that has the fault, which may be located on the fan side or on the load side of the motor. In this case, the calculation of the two-fault index (F2 and F3) is performed depending on the type of defect. These calculations are based on equations (1) and (2) previously described. Figure 11 shows the fault index calculation (F2) for ball faults

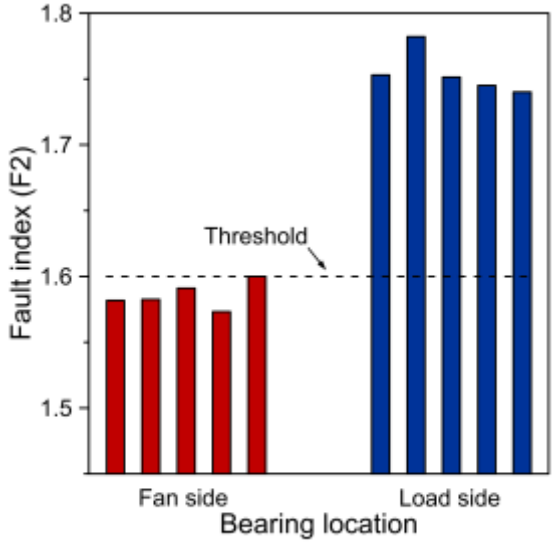

Figure 11. Criteria to define ball fault location.
Source: Authors, 2020.

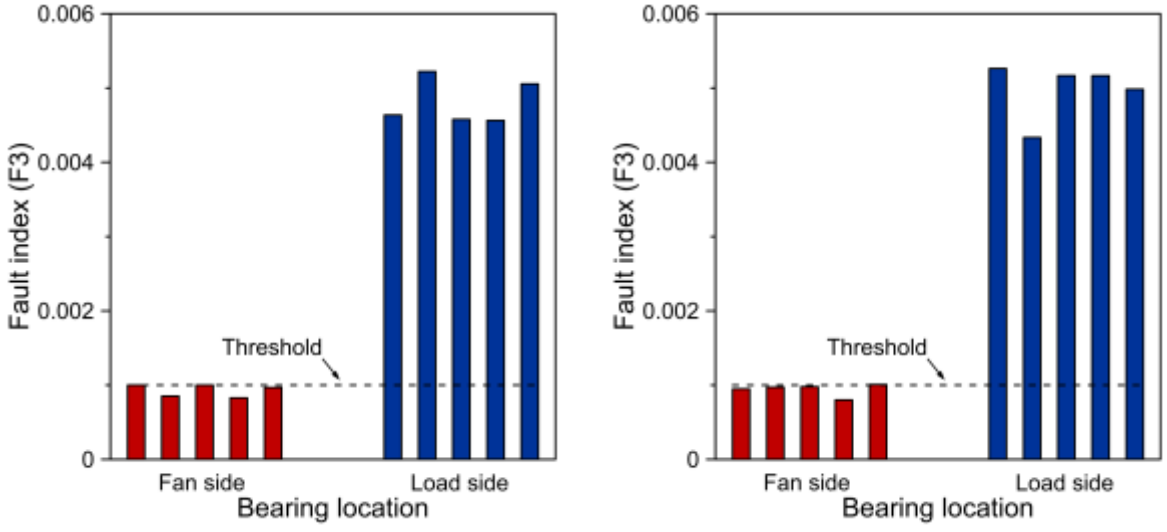

Figure 12. Criteria to define the location of (a) cage fault and (b) outer race fault.
Source: Authors, 2020.

The results obtained show that the bearings located on the fan sideshow appreciably less signal amplitude. This amplitude varied in a narrow range of 1.57-1.60. Therefore, the value of 1.60 was established as a threshold value that would allow defining the location of the faulty bearing. Similarly, the fault index calculation (F3) is used to locate bearings with cage faults and outer race faults. The results obtained are shown in Fig.12.

A behavior similar to that obtained in Fig.11 was observed. The signal amplitude is considerably greater for defective bearings located on the load side of the motor. In this case, a value of 0.001 can be considered as a threshold to locate the faulty bearing.

Conclusions

This article investigates a method of detecting, classifying, and locating the bearings of a three-phase induction motor that exhibits defects related to ball faults, cage faults, and outer race faults. The study method is based on an algorithm that analyzes the signals obtained from the Fast Fourier Transform and the Stockwell Transform. These signals were collected by measuring the current and voltage of the motor stator.

The characteristics of the electrical signals are strongly influenced by the presence of bearing faults. This can be verified by comparing the amplitudes of the signals calculated by FFT for a healthy and faulty condition. However, this type of analysis is not sufficient to detect defective bearings with high reliability. The results obtained show that, by calculating the difference between the total harmonic distortion of the current and voltage signal, it is possible to identify a threshold value of 0.004 that separates the healthy condition from the three fault states analyzed.

Using the Stockwell Transform, it is possible to generate a set of characteristics that can be classified using Fisher's Scoring Algorithm. The joint use of these two tools allows us to feed algorithms such as SVM to classify ball faults, cage faults, and outer race faults. With the use of this classification method, the accuracy of between 90% - 95% is achieved.

The maximum magnitude and maximum phase angle allow the location of the faulty bearing to be identified. In the case of the three faults studied, it was shown that the location of a bearing with defects on the load side generates a greater amplitude in the signal. This behavior allows establishing a threshold value of 1.6 for ball faults and 0.001 for cage faults and outer race. Due to the results obtained, it is concluded that the algorithm proposed in the study is a tool that can be used with a high degree of reliability for the diagnosis of the condition of the bearings.

Acknowledgment

The authors would like to acknowledge the Universidad del Atlántico and Sphere Energy company for their support in the development of this research.

References

[1] S. O. Gulhane and M. R. Salodkar, “Review of Detection of Faults in Induction Motor”, 2016.

[2] H. Arabaci and O. Bilgin, “Effects of rotor faults in squirrel-cage induction motors on the torque-speed curve”, in *The XIX International Conference on Electrical* Machines - ICEM 2010, pp. 1–5, 2010.

[3] D. V. Spyropoulos and E. D. Mitronikas, “A Review on the Faults of Electric Machines Used in Electric Ships”, *Advances in Power Electronics*, vol. 2013, pp. 1–8, 2013.

[4] M. A. Alsaedi, “Fault Diagnosis of Three-Phase Induction Motor: A Review”, *Optics*, vol. 4, no. 1, pp. 1, 2015.

[5] T. Aroui, Y. Koubaa, and A. Toumi, “Magnetic coupled circuits modeling of induction machines oriented to diagnostics”, *Leonardo Journal of Sciences*, vol. 7, no. 13, pp. 103–121, 2008.

[6] R. Moreno-Chuquen and O. Florez-Cediel, "Online Dynamic Assessment of System Stability in Power Systems Using the Unscented Kalman Filter", *International Review of Electrical Engineering (IREE*), vol. 14, no. 6, pp. 465–472, 2019.

[7] A. M. S. Yunus, M. Saini, M. R. Djalal, A. Abu-Siada, and M. A. S. Masoum, "Impact of Superconducting Magnetic Energy Storage Unit on Doubly Fed Induction Generator Performance During Various Levels of Grid Faults", *International Review of Electrical Engineering (IREE)*, vol. 14, no. 4, pp. 246–255, 2019.

[8] P. Thongprasri, "Investigation of a Switched Reluctance Generator Using the Voltage Pulse Width Modulation Method", *International Review of Electrical Engineering (IREE)*, vol. 13, no. 2, pp. 89–97, 2018.

[9] M. Widyan, "Operational Performance of Synchronous Generator Hybrid-Excited by PMDC and PV Generators", *International Review of Electrical Engineering (IREE)*, vol. 9, no. 4, pp. 863–872, 2014.

[10] M. S. Sepeeh, S. A. Zulkifli, S. Y. Sim, and E. Pathan, "A Comprehensive Review of Field-Oriented Control in Sensorless Control Techniques for Electric Vehicle", *International Review of Electrical Engineering (IREE)*, vol. 13, no. 6, pp. 461–475, 2018.

[11] K. C. Lakshmiah and T. A. Raghavendiran, "A New Modified H-Bridge Multilevel Inverter with Multi Carrier PWM Technique for Speed Control of Induction Motor", *International Review of Electrical Engineering (IREE)*, vol. 13, no. 5, pp. 365–372, 2018.

[12] Ç. Acar, O. C. Soygenc, and L. T. Ergene, "Increasing the Efficiency to IE4 Class for 5.5 kW Induction Motor Used in Industrial Applications", *International Review of Electrical Engineering (IREE)*, vol. 14, no. 1, pp. 67–78, 2019.

[13] F. S. El-Faouri, O. Mohamed, and W. A. Elhaija, "Model-Based Field-Oriented Control of a Three-Phase Induction Motor with Consideration of Rotor Resistance Variation", *International Review of Electrical Engineering (IREE)*, vol. 14, no. 3, pp. 173–181, 2019.

[14] M. A. Mossa and A. A. Z. Diab, "Effective Model Predictive Control Approach for a Faulty Induction Motor Drive", *International Review of Electrical Engineering (IREE)*, vol. 14, no. 5, pp. 314–327, 2019.

[15] H. H. Hanafy, T. M. Abdo, and A. A. Adly, "2D finite element analysis and force calculations for induction motors with broken bars", *Ain Shams Engineering Journal*, vol. 5, no. 2, pp. 421–431, 2014.

[16] M. Akar and I. Cankaya, "Broken rotor bar fault detection in inverter-fed squirrel cage induction motors using stator current analysis and fuzzy logic", *Turkish Journal of Electrical Engineering and Computer Sciences*, vol. 20, pp. 1077–1089, 2012.

[17] M. A. Juneghani, B. K. Boroujeni, and M. Abdollahi, "Determination of number of broken rotor bars in squirrel-cage induction motors using adaptive neuro-fuzzy interface system", *Research Journal of Applied Sciences, Engineering and Technology*, vol. 4, pp. 3399–3405, 2012.

[18] T. C. Anil Kumar, G. Singh, and V. N. A. Naikan, "Effectiveness of vibration monitoring in the health assessment of induction motor", *International Journal of Prognostics and Health Management*, vol. 6, pp. 1–9, 2015.

[19] Y. Liu and A. M. Bazzi, "A review and comparison of fault detection and diagnosis methods for squirrel-cage induction motors: State of the art", *ISA Transactions*, vol. 70, pp. 400–409, 2017.

[20] İ. Y. önel, K. Burak Dalci, and İ. Senol, "Detection of outer raceway bearing defects in small induction motors using stator current analysis", *Sadhana*, vol. 30, no. 6, pp. 713–722, 2005.

[21] S. E. Pandarakone, Y. Mizuno, and H. Nakamura, "Distinct Fault Analysis of Induction Motor Bearing Using Frequency Spectrum Determination and Support Vector Machine", *IEEE Transactions on Industry Applications*, vol. 53, no. 3, pp. 3049–3056, 2017.

[22] R. H. C. Palácios, I. N. da Silva, A. Goedtel, and W. F. Godoy, "A novel multi-agent approach to identify faults in line connected three-phase induction motors", *Applied Soft Computing*, vol. 45, pp. 1–10, 2016.

[23] A. Rai and S. H. Upadhyay, "A review on signal processing techniques utilized in the fault diagnosis of rolling element bearings", *Tribology International*, vol. 96, pp. 289–306, 2016.

[24] E. Elbouchikhi, V. Choqueuse, Y. Amirat, M. E. H. Benbouzid, and S. Turri, "An Efficient Hilbert–Huang Transform-Based Bearing Faults Detection in Induction Machines", *IEEE Transactions on Energy Conversion*, vol. 32, no. 2, pp. 401–413, 2017.

[25] M. Lopez-Ramirez et al., "Detection and diagnosis of lubrication and faults in bearing on induction motors through STFT, in 2016 International Conference on Electronics", *Communications and Computers (CONIELECOMP)*, 2016, pp. 13–18.

[26] O. P. Mahela and A. G. Shaik, "Recognition of power quality disturbances using S-transform based ruled decision tree and fuzzy C-means clustering classifiers", *Applied Soft Computing*, vol. 59, pp. 243–257, 2017.

[27] O. P. Mahela and A. G. Shaik, "Power quality recognition in distribution system with solar energy penetration using S -transform and Fuzzy C-means clustering", *Renewable Energy*, vol. 106, pp. 37–51, 2017.

[28] M. Singh and A. G. Shaik, "Application of stockwell transform in bearing fault diagnosis of induction motor", in *2016 IEEE 7th Power India International Conference (PIICON*), pp. 1–6, 2016.